Polymer 49 (2008) 5387–5396

Contents lists available at ScienceDirect

Polymer

journal homepage: www.elsevier.com/locate/polymer

Synthesis and characterization of poly(arylene ether sulfone)-*b*-polybenzimidazole copolymers for high temperature low humidity proton exchange membrane fuel cells

Hae-Seung Lee, Abhishek Roy, Ozma Lane, James E. McGrath*

Chemistry Department, Macromolecules and Interfaces Institute (MII), and Institute for Critical Technology and Applied Science (ICTAS), Virginia Polytechnic Institute and State University, Blacksburg, VA 24061, United States

ARTICLE INFO

Article history:
Received 17 May 2008
Received in revised
form 12 September 2008
Accepted 14 September 2008
Available online 26 September 2008

Keywords:
Multiblock copolymer
Poly(arylene ether sulfone)
Polybenzimidazole

ABSTRACT

Multiblock copolymers based on poly(arylene ether sulfone) and polybenzimidazole (PBI) with different block lengths were synthesized by coupling carboxyl functional aromatic poly(arylene ethers) with ortho diamino functional PBI oligomers in NMP, selectively doped with phosphoric acid, and evaluated as a high temperature proton exchange membrane (PEM). Transparent and ductile membranes were produced by solvent casting from DMAc. From dynamic mechanical analysis (DMA), the neat copolymer membranes showed two distinct glass transition temperatures which implies the existence of a nano-structured morphology in the membranes. These two nanophases became more distinct with increasing block length. The membranes were immersed in various concentrations of phosphoric acid solution to produce the proton conductivity. The doping level increased with increasing concentration of the acid solution and a maximum doping level of 12 was achieved when 14.6 M phosphoric acid solution was used. The acid doped membranes showed significantly reduced swelling behavior compared to a control conventional phosphoric acid doped PBI homopolymer system which appears to be related to the selective sorption into the PBI phase. The ionic conductivity of the doped samples at 200 °C afforded up to 47 mS/cm without external humidification. The protonic conductivity was found to increase with block length at a given doping level, reflecting the sharpness of the nanophase separation and the effect was even more prominent at a low doping level of 6–7. It is suggested that the phosphoric acid doped multiblock copolymer system would be a strong candidate for high temperature and low relative humidity PEM applications such as those required for stationary power.

1. Introduction

The fuel cell is well known to be an energy conversion device which transforms chemical energy directly into electrical energy [1]. Its high energy efficiency and environmentally friendly nature have attracted much attention, making the fuel cell an alternative to conventional energy sources. Among several types of fuel cells, polymer electrolyte membrane fuel cells (PEMFCs) have been most intensively explored for past decades due to their promise for mobile, automotive, and stationary applications [2]. The state-of-the-art PEMs are perfluorinated sulfonic acid containing ionomers (PFSAs) which have demonstrated excellent performances including high proton conductivity and excellent chemical stability [3,4]. However, their mechanical and electrochemical properties deteriorate [5] at higher operating temperatures and low relative humidity (RH) conditions since the proton transport of sulfonic acid based PEMs strongly depends on water in the membranes. It has been proposed that the proton conduction of the sulfonic acid containing PEMs is governed by a vehicle mechanism, where water acts as the vehicle for proton transport [6]. Hence at high temperature and at very low RH, the proton transport is restricted due to insufficient water. Consequently, various approaches have been made to develop PEMs which are suitable for high temperature under low RH conditions.

One of the successful high temperature, low RH PEMs is well recognized to be an inorganic acid doped polymer membrane system [7–10]. The inorganic acids act as ion conducting materials while polymers, which typically possess basic moieties, can immobilize the acid. Among various inorganic acids, phosphoric acid (H_3PO_4) has been widely studied due to its excellent thermal stability, low vapor pressure, and high ionic conductivity even under anhydrous conditions [11–15]. For the matrix polymer, the polybenzimidazole (PBI) family, especially poly(2,2′-*m*-(phenylene)-5,5′-bibenzimidazole), has been intensively studied due to the ease of synthesis and commercial availability [16,17]. Phosphoric

* Corresponding author. Tel.: +1 540 231 5976; fax: +1 540 231 8517.
E-mail address: jmcgrath@vt.edu (J.E. McGrath).

0032-3861/$ – see front matter © 2008 Elsevier Ltd. All rights reserved.
doi:10.1016/j.polymer.2008.09.019

acid doped PBI membranes can be easily fabricated by immersing solvent cast PBI membranes in phosphoric acid solution. The doping level which can be defined as the number of moles of phosphoric acid per one repeat unit of PBI is controlled by using different concentrations of the doping solution [18]. More recently, Benicewicz et al. have elegantly shown that one can directly polymerize and cast from polyphosphoric acid (PPA). The controlled hydrolysis of PPA in the film affords very large doping levels and excellent performance [19].

In contrast to sulfonic acid based PEMs, the ion transport in phosphoric acid doped systems under anhydrous conditions is thought to follow a proton hopping or Grotthus mechanism [20,21]. The mechanism is reported to depend strongly on acid doping level, water content and temperature. At low doping levels, the proton transport has been suggested to take place between the N–H sites of the polymer and phosphate anion. At higher doping levels, the presence of "free" acid facilitates the enhanced transport from the more rapid diffusion of additional phosphate anions [22]. In the presence of water, ions such as H_3O^+ also can be involved as an additional proton carrier. At high temperatures in the condensed phosphoric acid state, ion transport involving protonic diffusion via the vehicle mechanism is also proposed [23].

Generally, the ionic conductivity of phosphoric acid doped PBI homopolymers increases along with doping level and temperature. However, doping levels higher than 5 may not be desirable in current commercial PBI due to high swelling and deterioration of mechanical properties [24]. Although several approaches have been attempted to address this problem, such as crosslinking of the matrix polymer [25,26], and introducing inorganic fillers to reinforce the membrane [27], highly doped membranes still suffer from mechanical property deterioration, a perceived and perhaps actual problem with electrode performance.

Similar trade-off behaviors between proton conductivity and dimensional stability have been observed in sulfonic acid containing PEM systems. Although an increased degree of sulfonation in the system enhances proton conductivity, beyond a certain concentration a percolated hydrophilic phase develops resulting in excessive water swelling, and a hydrogel which is impractical as a PEM [28,29]. Recently, these problems have been successfully addressed by utilizing multiblock copolymers based on ion conducting hydrophilic blocks and mechanically robust hydrophobic blocks [30–34]. Once the block copolymers are cast into membranes, they can exhibit unique phase separated morphologies and each phase governs independent properties. The ionic groups of the hydrophilic blocks act as proton conducting sites while the nonionic hydrophobic component provides dimensional stability.

In the present work, multiblock copolymers were produced by a homogeneous coupling reaction in NMP between highly reactive *o*-diamino functional PBI oligomers and carboxylic acid-terminated poly(arylene ether sulfone) oligomers [35]. The latter was prepared by using *m*-hydroxybenzoic acid as an efficient end-capper during the nucleophilic step polymerization. The carboxylate formed is unreactive but the phenoxy anion is quite reactive with the activated aromatic halide. The PBI segments in the system facilitate ionic conduction by providing a selective site for absorption of H_3PO_4 while poly(arylene ether sulfone) segments are unaffected and maintain the dimensional and mechanical stability. Ionic transport measurements on the copolymers have been investigated in the absence and in the presence of water as a function of doping level, temperature and morphology.

2. Experimental

2.1. Materials

N,*N*-Dimethylacetamide (DMAc), *N*-methyl-2-pyrrolidinone (NMP), and toluene were purchased from Aldrich and distilled from calcium hydride before use. Monomer grade 4,4′-dichlorodiphenyl sulfone (DCDPS) and 4,4′-biphenol (BP) were provided by Solvay Advanced Polymers and Eastman Chemical Company, respectively, and vacuum dried at 110 °C prior to use. Potassium carbonate, 3-hydroxybenzoic acid (99%) (3-HBA), isophthalic acid (99%), 3,3′-diaminobenzidine (99%) (DAB), phosphoric acid (85%) and polyphosphoric acid (115%) were purchased from Aldrich and used without further purification.

2.2. Synthesis of controlled molecular weight poly(arylene ether sulfone)s with telechelic benzoic acid functionality

Benzoic acid-terminated poly(arylene ether sulfone) oligomers (BPS) with molecular weights of 5, 10, and 15 kg/mol were synthesized. An example of the synthesis of 5 kg/mol BPS is as follows: 10.6730 g (57.3 mmol) of BP, 17.9209 g (62.4 mmol) of DCDPS, 1.4061 g (10.2 mmol) of 3-HBA and 11.1900 g (81.0 mmol) of potassium carbonate were added to a three-neck 250-mL flask equipped with a condenser, a Dean Stark trap, a nitrogen inlet/outlet, and a mechanical stirrer. Distilled DMAc (120 mL) and toluene (60 mL) were added to the flask. The solution was allowed to reflux at 155 °C while the toluene azeotropically removed the water from the system. After 4 h, the toluene was completely removed from the system and the reaction temperature was increased to 180 °C. The reaction was allowed to proceed for another 48 h. The resulting viscous solution was filtered to remove the salts and coagulated in methanol. The telechelic benzoic acid functionality of the oligomer was recovered from its potassium salt form by stirring the coagulated polymer in 0.1 M aqueous sulfuric acid solution for 24 h. The polymer was dried at 110 °C *in vacuo* for at least 24 h.

2.3. Synthesis of controlled molecular weight diamine-terminated polybenzimidazole

Diamine-terminated polybenzimidazole blocks with molecular weight 5, 10, and 15 kg/mol were synthesized. A typical coupling reaction was performed as follows: 5.8977 g (35.5 mmol) of isophthalic acid and 8.0995 g (37.8 mmol) of DAB were mixed with 126 g of polyphosphoric acid in a three-neck 250-mL flask equipped with a nitrogen inlet/outlet and a mechanical stirrer. The mixture was heated at 200 °C for 24 h. The resulting dark brown polymer solution was coagulated in deionized water and stirred for 24 h. The telechelic oligomer was filtered and washed with deionized water several times. The residual acid in the polymer was neutralized with 1 M NaOH solution. It was dried at 120 °C *in vacuo* for at least 24 h.

2.4. Synthesis of poly(arylene ether sulfone)-b-polybenzimidazole multiblock copolymers

Multiblock copolymers were synthesized via a coupling reaction between the benzoic acid and *o*-diamino end groups on the poly(arylene ether sulfone) and polybenzimidazole oligomers, respectively. A typical coupling reaction was performed as follows: 3.0000 g (0.6 mmol) of poly(arylene ether sulfone) oligomer ($\overline{M}_n$ = 5 kg/mol), 3.0000 g (0.6 mmol) of polybenzimidazole oligomer ($\overline{M}_n$ = 5 kg/mol) and 60 mL of NMP were added to a three-neck 100-mL flask equipped with a mechanical stirrer, and a nitrogen inlet/outlet. The reaction mixture was heated at 200 °C and allowed to proceed for 48 h. The resulting dark brown viscous copolymer solution was precipitated in methanol and filtered. The polymer was dried at 120 °C *in vacuo* for at least 24 h.

2.5. Characterization of copolymers

^{1}H NMR analyses were conducted on a Varian INOVA 400 MHz spectrometer with DMSO-d_6 or DMAc-d_9 to confirm the chemical

structures of oligomers and copolymers. ^{1}H NMR spectroscopy was also used to determine copolymer compositions and number-average molecular weights of the oligomers via end group analyses. Intrinsic viscosities were determined in NMP at 25 °C using an Ubbelohde viscometer. Dynamic mechanical analysis was performed on a TA DMA 2980 using a thin film tension clamp in order to characterize the thermal properties of the multiblock copolymers. After heating to 220 °C to evaporate any remaining trace amounts of solvent, the samples were then equilibrated for 10 min at 0 °C under nitrogen and heated at a rate of 3 °C/min to 450 °C, using an oscillation of 1 Hz.

2.6. Film casting and H_3PO_4 doping

Multiblock copolymer membranes were prepared by solution casting from DMAc. The copolymers were dissolved in DMAc (10% w/v), filtered through 0.45 μm Teflon® syringe filters, and cast onto clean glass substrates. The solvent was evaporated under an infrared lamp for 48 h at 50–70 °C, resulting in transparent, tough, and flexible films. The films were further dried *in vacuo* at 110 °C for 24 h to remove residual solvent. The H_3PO_4 doped membranes were prepared by immersing the cast membranes in a various concentrations (3–14.6 M) of aqueous H_3PO_4 solution for 72 h at room temperature.

2.7. Determination of doping level, water uptake, and swelling ratio

The doping level and water uptake of the H_3PO_4 doped membranes were determined by weight comparisons between undoped, doped, and vacuum dried doped membranes. First, the DMAc cast membranes were dried at 150 °C *in vacuo* for 24 h and their weights (W_{dry}) were recorded. The dried membranes were then immersed in H_3PO_4 solutions. After 72 h, the membranes were taken out, wiped dry, and weighed (W_{wet}). Finally, the membranes were dried in a vacuum oven at 110 °C for 24 h and weighed (W_{acid}).

$$\text{Weight Increase}(\%) = \frac{W_{wet} - W_{dry}}{W_{dry}} \times 100$$

$$\text{Weight uptake}(\%) = \frac{W_{wet} - W_{acid}}{W_{dry}} \times 100$$

$$\text{Doping level} = \frac{\left(W_{acid} - W_{dry}\right)/MW_{PA}}{\left(W_{dry} \times F_{PBI}\right)/MW_{PBI}}$$

where MW_{PA} and MW_{PBI} represent the molecular weights of phosphoric acid and repeat unit of PBI, respectively. F_{PBI} is the fraction of PBI portion in the multiblock copolymer (e.g., %PBI composition divided by 100).

The swelling ratios of copolymers were determined as follows

$$\text{Swelling ratio}(\%) = \frac{\left(l_{wet} - l_{dry}\right)}{l_{dry}} \times 100$$

where l_{dry} and l_{wet} represent the length or thickness of dry and wet films, respectively.

2.8. Determination of ionic conductivity

All conductivity measurements were made using a Solartron (1252A +1287) impedance/gain-phase analyzer over the frequency range of 10 Hz–1 MHz. The conductivity of the membrane was determined from the geometry of the cell and resistance of the film which was taken at the frequency that produced the minimum imaginary response. For the temperature sweep experiments, the conductivity cells with the membranes were equilibrated at 100 °C for 4–5 h before the start of the experiment. This was done to remove the excess water from the membranes. In situ measurements were taken as a function of increasing temperature with the cells equilibrated in a convection oven. Equilibration time at each temperature was kept fixed at 3 h.

3. Results and discussion

3.1. Synthesis of poly(arylene ether sulfone) and polybenzimidazole oligomers

Carboxylic acid-terminated poly(arylene ether sulfone) oligomers (BPS) whose molecular weights range from 5 to 15 kg/mol were synthesized via step-growth polymerization of DCDPS, BP, and 3-HBA (Fig. 1). Telechelic benzoic acid functionality of the oligomers was achieved by utilizing 3-HBA as an end-capping agent as reported earlier [35]. Molecular weights of the oligomers were controlled by using stoichiometrically adjusted amounts of monomers and end-capping reagent. The number-average molecular weights of the BPS oligomers were determined by end group analysis of the ^{1}H NMR spectra. The peak at 7.61 ppm was assigned to one of the protons on the benzoic acid end group while the peak at 7.71 ppm was assigned to the protons on the phenyl ring in the main polymer backbone (Fig. 2). By comparing the integrations of both peaks, the number-average molecular weights of the BPS oligomers were determined (Table 1).

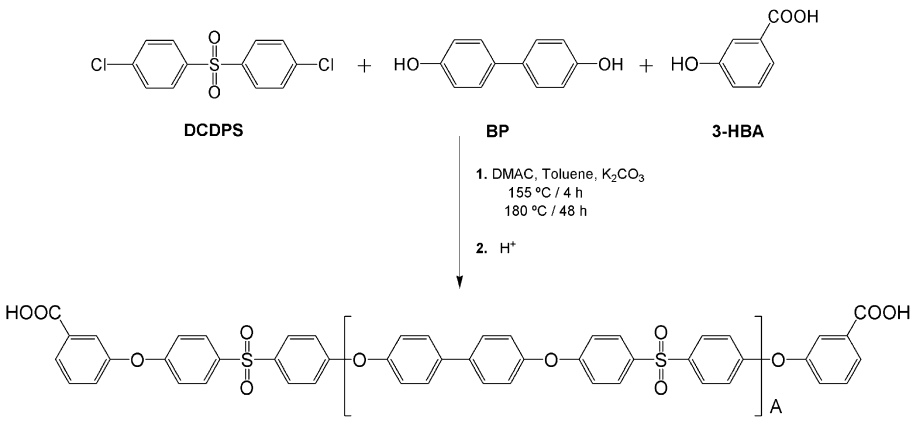

Fig. 1. Synthesis of a benzoic acid-terminated poly(arylene ether sulfone) oligomer.

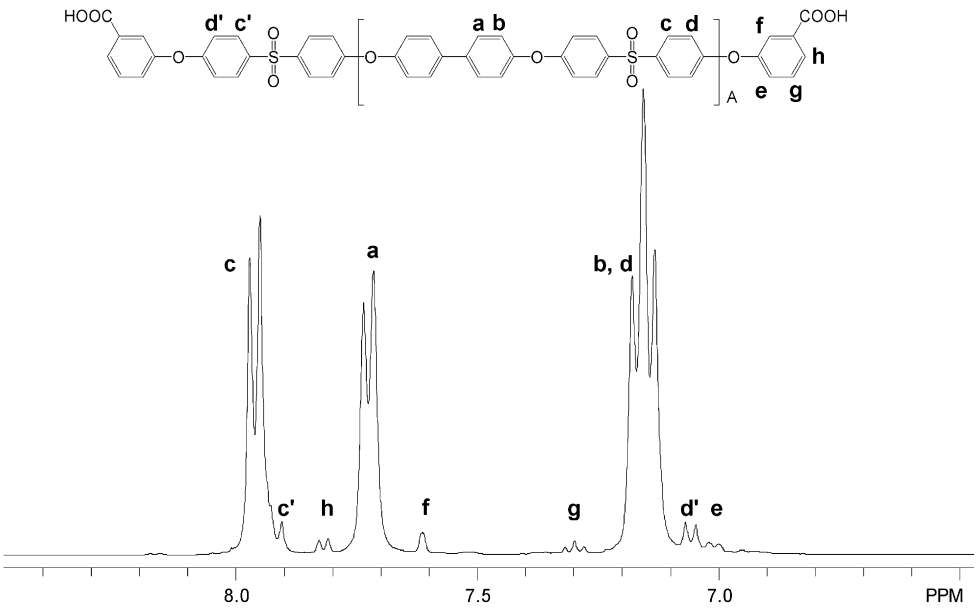

Fig. 2. ^{1}H NMR spectrum of a benzoic acid-terminated poly(arylene ether sulfone) oligomer.

o-Diamino-terminated polybenzimidazole oligomers (PBI) with the same molecular weight of BPS oligomers were synthesized via step-growth polymerization in polyphosphoric acid (Fig. 3). The molecular weight and diamine end group functionality of the oligomers were controlled by offsetting monomer stoichiometry. The number-average molecular weight of each PBI oligomer was determined from the ^{1}H NMR spectrum. The peaks ranging from 6.5 to 7.0 ppm and from 12.8 to 13.5 were assigned to the protons on the *o*-diamino benzene moieties and the amine protons on benzimidazole moieties, respectively (Fig. 4). By comparing the integrals, number-average molecular weights were determined and are summarized in Table 1.

Intrinsic viscosities of both BPS and PBI oligomers were measured in NMP by using a Ubbelohde viscometer. As expected, increased viscosities were observed with increasing molecular weight. In addition, when the viscosities of the oligomers were plotted with the determined number-average molecular weights in a log–log scale, a linear relationship was observed for both BPS and PBI oligomers which confirmed the successful control of molecular weight for both the block series (Figs. 5 and 6).

Table 1
Characterization of BPS and PBI telechelic oligomers

Target M_n (g mol^{-1})	BPS oligomer		PBI oligomer	
	M_n (g mol^{-1})[a]	IV (dL g^{-1})[b]	M_n (g mol^{-1})[a]	IV (dL g^{-1})[b]
5000	5400	0.22	5400	0.58
10,000	9800	0.38	11,700	1.23
15,000	14,700	0.55	16,100	1.64

[a] Determined by ^{1}H NMR end group analyses.
[b] In NMP at 25 °C.

3.2. Synthesis of BPS–PBI multiblock copolymers

The multiblock copolymers were synthesized by a coupling reaction between BPS and PBI oligomers of equal block length in NMP. The coupling reaction was achieved by forming benzimidazole moieties between benzoic acid and *o*-diamino end groups on the BPS and PBI oligomers, respectively (Fig. 7). For the coupling reaction, polyphosphoric acid was initially considered as a reaction solvent. However, poor solubility of BPS oligomers made the coupling reaction impossible in polyphosphoric acid. For this reason, the coupling reactions of BPS and PBI oligomers were performed in NMP, which dissolved both BPS and PBI oligomers. Since high molecular weight multiblock copolymers can be readily synthesized from several oligomers of sufficient length, NMP served as a good solvent to conduct the coupling reaction. The ^{1}H NMR spectrum of the BPS–PBI copolymer showed the disappearance of the end group peaks of both BPS and PBI oligomers, which confirmed that the block copolymerization was successful (Fig. 8). In addition, ^{13}C NMR experiments also showed the disappearance

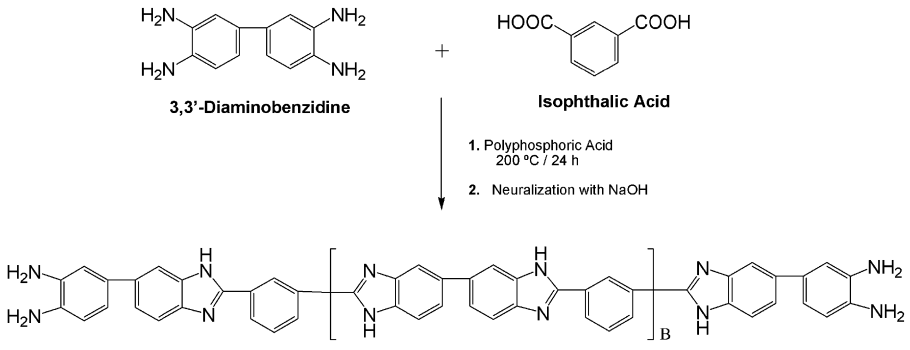

Fig. 3. Synthesis of a *o*-diamino-terminated polybenzimidazole oligomer.

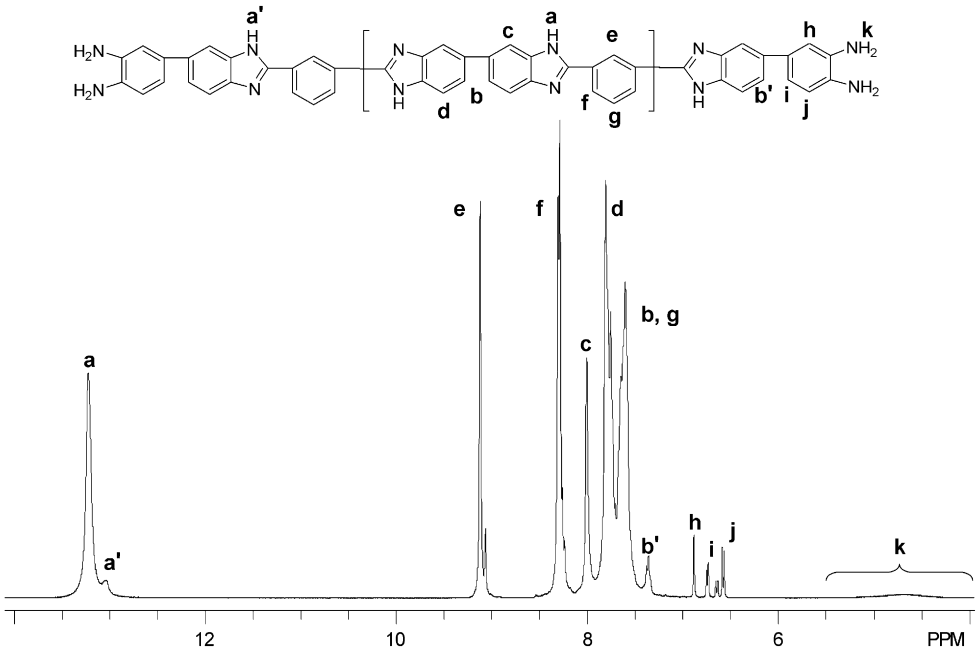

Fig. 4. ^{1}H NMR spectrum of a diamine-terminated polyimide hydrophobic oligomer.

of the carbonyl carbon peak from the BPS oligomer after the coupling reaction.

3.3. Characterization of the BPSH–PBI multiblock copolymers

The chemical composition of the copolymers was calculated by comparing the peak integrations from each oligomer on ^{1}H NMR spectra. The determined chemical compositions of PBI in the copolymer varied from 45 to 47%, which were slightly lower than the feed value (e.g., 50%). The intrinsic viscosities of the copolymers ranged from 0.78 to 1.91 dL g^{-1} (Table 2). All copolymers produced tough, ductile membranes when solvent cast from DMAc. DMA analysis showed that with increasing block length, the two glass transition peaks attributed to the separate BPS and PBI regimes became increasingly distinct (Fig. 9). While the PBI transition of 333–337 °C remained constant, the BPS transition shifted from 215 °C to 191 °C. This implies a lower level of a mixed-regime phase as higher block lengths allowed a greater degree of phase separation. The upper T_g from the E' drop seems a bit low, which may be a segment M_n issue, but the tan delta loss seems to be about what one would have expected.

3.4. Water uptake, H_3PO_4 doping level, and swelling ratio

The copolymers were soluble in DMAc without any insoluble residue and produced transparent and ductile membranes. Acid doped copolymer membranes were prepared using various concentrations of H_3PO_4 solution. First, to determine the time required to saturate the copolymer membranes in different concentrations of H_3PO_4 solution, the membranes were immersed in 3, 9, and 14.6 M H_3PO_4 solutions and their weight gains were measured as a function of time. Fig. 10 shows the weight increase behavior of BPS10–PBI10 with different acid concentrations. As can be seen from the figure, a higher concentration of doping solution reduces the time to saturate the film with H_3PO_4. With the 3 M H_3PO_4 solution, at least 24 h was necessary to saturate the membrane while only 6 h was adequate for the 14.6 M H_3PO_4 solution. Based on the results, further doping experiments were performed for 72 h to obtain the maximum acid doping level.

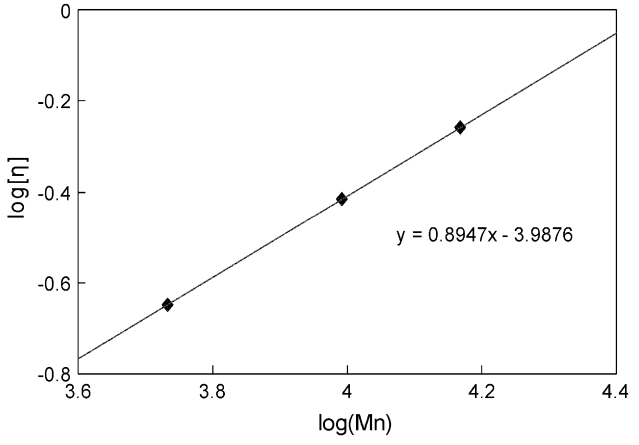

Fig. 5. Double logarithmic plot of [η] versus M_n of poly(arylene ether sulfone) oligomers.

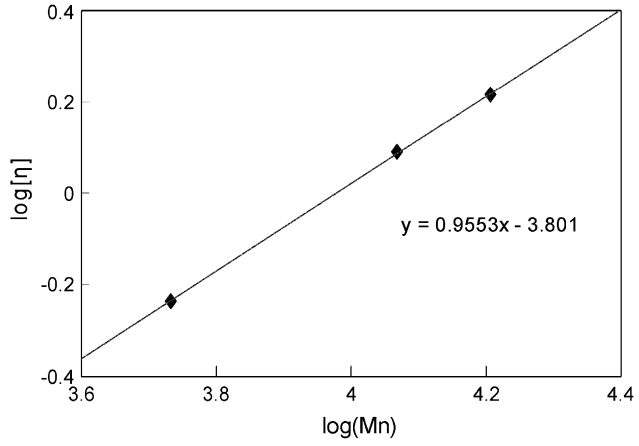

Fig. 6. Double logarithmic plot of [η] versus M_n of polybenzimidazole oligomers.

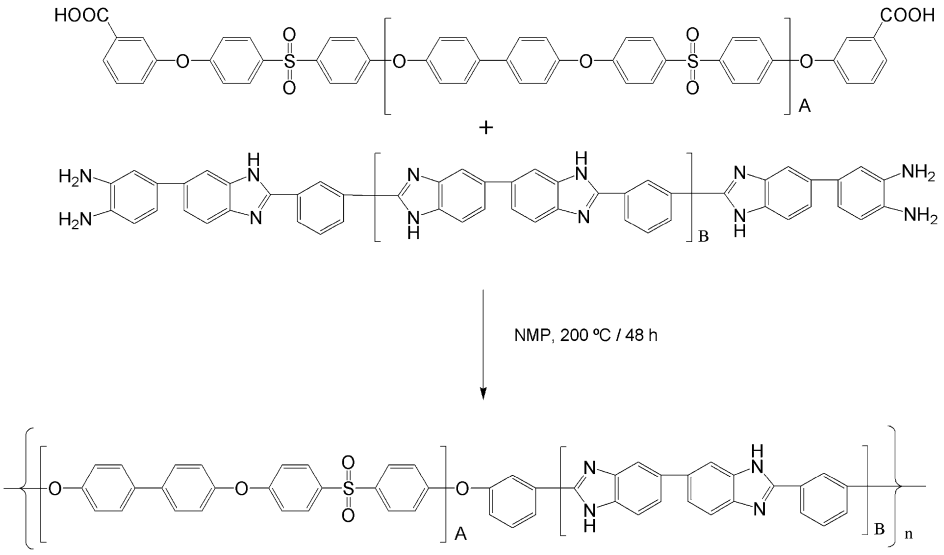

Fig. 7. Synthesis of a poly(arylene ether sulfone)-*b*-polybenzimidazole (BPS–PBI) copolymer.

To determine the doping level and water uptake, a series of BPS–PBI copolymers with different block lengths was immersed in different concentrations of H_3PO_4 solution. After 72 h of immersion in the acid solutions, their weight increases were measured and plotted as a function of the doping concentration (Fig. 11). As expected, larger weight gains were observed for higher concentrations of doping solutions. However, no significant variation of weight increase was observed with changes of block lengths.

The weight increases of acid doped membranes can be attributed both to imbibed H_3PO_4 and water. To evaluate the contribution of each factor in the weight increase, the acid doped membranes were dried in a vacuum oven at 110 °C for 24 h. The drying process selectively removed water out of the membrane without the condensation of H_3PO_4 in the membranes. The weight loss after the drying was interpreted as the water uptake of the sample while remaining weight increase was considered as the weight of H_3PO_4 by the doping process. Fig. 12 shows the contribution of the water uptake and the acid doping for the weight increases. Interestingly, as the concentration of acid doping solution increased, the water uptake of the copolymers remained similar while the weight increases by acid were significant. This behavior is well matched with the earlier study which was performed by Bjerrum et al. [18].

The doping levels of the membranes were also determined (Fig. 13). The doping levels increased linearly with increasing solution concentration up to 12 M. However, when the concentration was higher than 12 M, the doping level increased more rapidly and reached 12 for the 14.6 M acid concentration. It is noteworthy that the doped copolymer membranes showed limited swelling ratios even at high doping levels. For H_3PO_4 doped conventional PBI homopolymer membranes, it has been generally accepted that the doping level 5 is the highest value for practical applications without any observed deterioration of mechanical strength and ionic conductivity [18]. However, when BPS–PBI and PBI homopolymer membranes were immersed in 14.6 M H_3PO_4 solution for 72 h, the BPS–PBI membranes with high doping levels (e.g., 9.65–12.02) showed less than 4% in-plane and 60% through-plane swelling ratios while PBI homopolymer exhibited 22% and 105% swelling ratios, respectively (Table 3). This result is not surprising if we consider that the acid contents of the doped multiblock copolymer membranes (e.g., 59–63 wt.%) are lower than that of the homopolymer PBI (78 wt.%). To compare the swelling behaviors of the two systems with similar acid contents, a homopolymer PBI membrane with 60.9% acid content was also fabricated by immersion in 12 M H_3PO_4 solution. Although the acid content of the

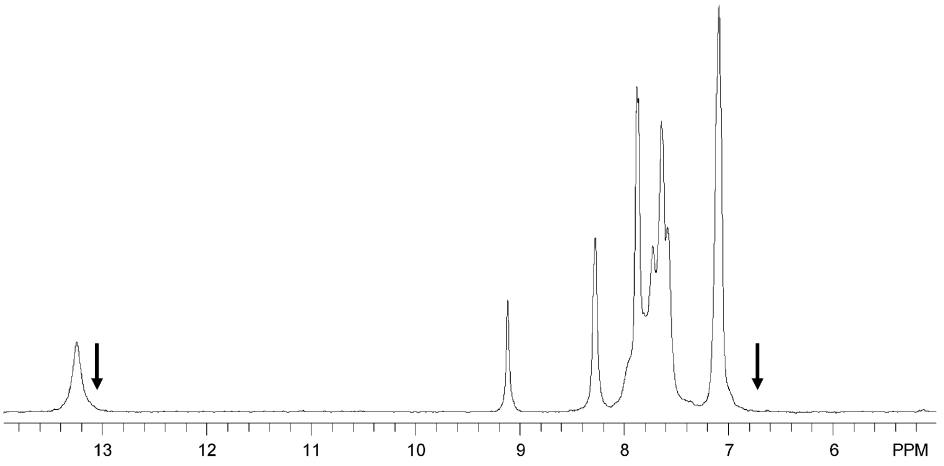

Fig. 8. ^{1}H NMR spectrum of a BPS–PBI multiblock copolymer. Black arrows represent the disappearance of the diamine end groups on the PBI blocks after the coupling reaction with benzoic acid-terminated BPS blocks.

Table 2
Characterization of BPS *x*–PBI *y*[a] copolymers

Copolymers (BPS/PBI) (%) (dL g^{-1})[c]	Copolymer composition[b]	IV	T_g (°C)[d]	
			1st	2nd
BPS 5–PBI 5	54/46	0.78	215	337
BPS 10–PBI 10	53/47	1.00	204	333
BPS 15–PBI 15	55/45	1.91	191	336

[a] Acronym for copolymers (BPS *x*–PBI *y*): *x* = molecular weight of the poly(arylene ether sulfone) block (BPS) in units of kg/mol; *y* = molecular weight of the polybenzimidazole block (PBI) in units of kg/mol.
[b] Determined by ^{1}H NMR.
[c] In NMP at 25 °C.
[d] Measured by DMA; *E′*, modulus drop.

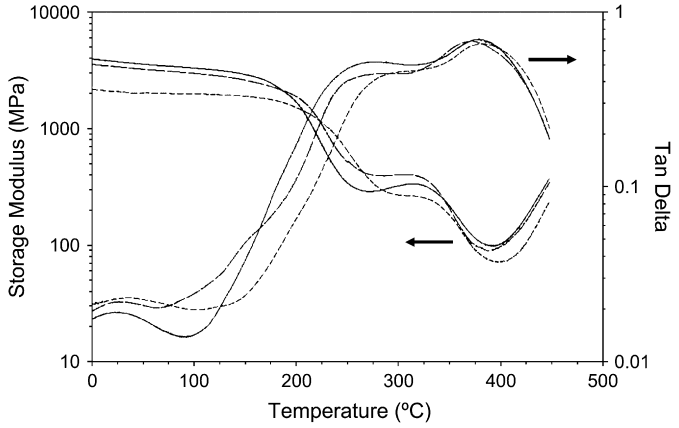

Fig. 9. Storage modulus and tan delta curves for BPS–PBI copolymers. Short dash line, long dash line, and solid line represent BPS5–PBI5, BPS10–PBI10, and BPS15–PBI15, respectively.

homopolymer PBI membrane was reduced to 60.9% to match the acid contents of multiblock copolymers, the PBI homopolymer membrane still showed much a higher swelling ratio than those of multiblock copolymers. A possible explanation of the low swelling ratios of the multiblock copolymers might be the selective doping of the acid in the multiblock copolymer membranes. Since poly(arylene ether sulfone) BPS segments do not absorb phosphoric acid, the doped phosphoric acid mainly exists in the PBI segments while the poly(arylene ether sulfone) segments maintain physical integrity and reduce the swelling ratios even with high doping levels. Hence, the low swelling ratios and minor softening of the

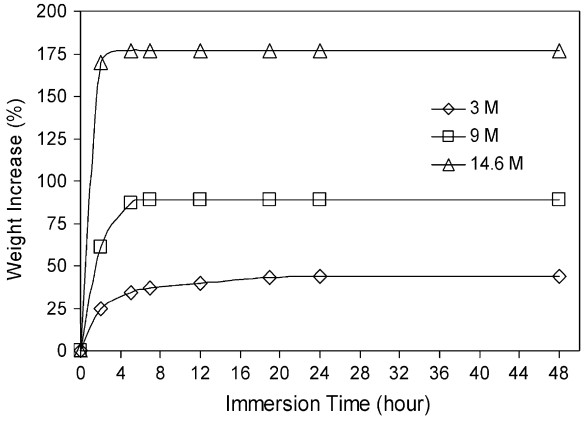

Fig. 10. Weight gains of BPS10–PBI10 as a function of immersion time with different acid concentrations.

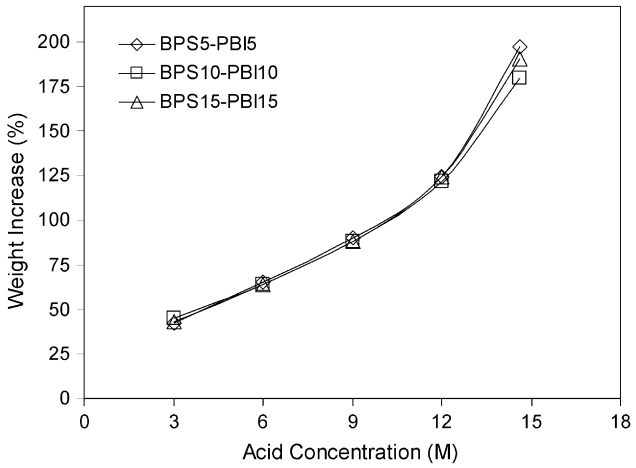

Fig. 11. Weight increases of BPS–PBI membranes as a function of the acid concentration with different block lengths.

acid doped multiblock copolymer membranes suggest that higher doping levels (e.g., >6) could be utilized to further enhance the ionic conductivities without any significant deterioration of the mechanical strength. Detailed mechanical properties of BPS15–PBI15 with different doping levels are summarized in Table 4.

3.5. Influence of temperature and doping levels of phosphoric acid on ionic conductivity

The ionic conductivities of the BPS–PBI copolymers were determined as a function of temperature without any external humidification supply. The temperature range was 100–200 °C. Fig. 14 represents the temperature vs. conductivity plot for BPS5–PBI5 doped with different concentrations of phosphoric acid (e.g., 3, 9, 12, and 14.6 M). A similar study was conducted for BPS10–PBI10 and BPS15–PBI15 samples as shown in Figs. 15 and 16. The numbers within the brackets in the legends refer to the doping levels of the samples.

In all cases, the ionic conductivities increased with increasing temperature and doping levels. However, the conductivities of the copolymers doped at higher concentrations (e.g., 12 and 14.6 M) increased more rapidly with temperature than in samples doped with lower concentrations (e.g., 3 and 9 M). For the membranes

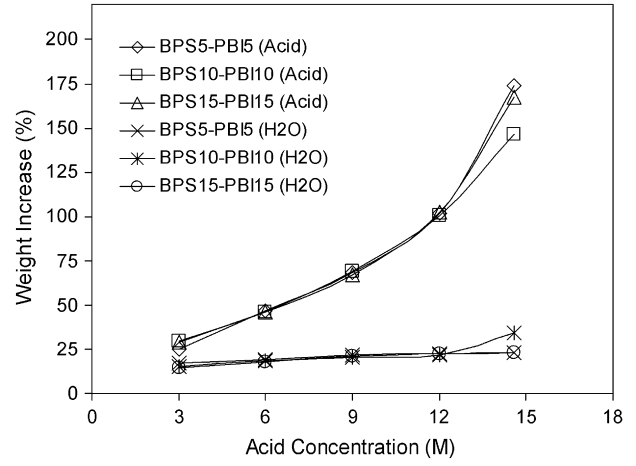

Fig. 12. Contribution of phosphoric acid and water to the weight increases of BPS–PBI membranes as a function of the acid concentration with different block lengths.

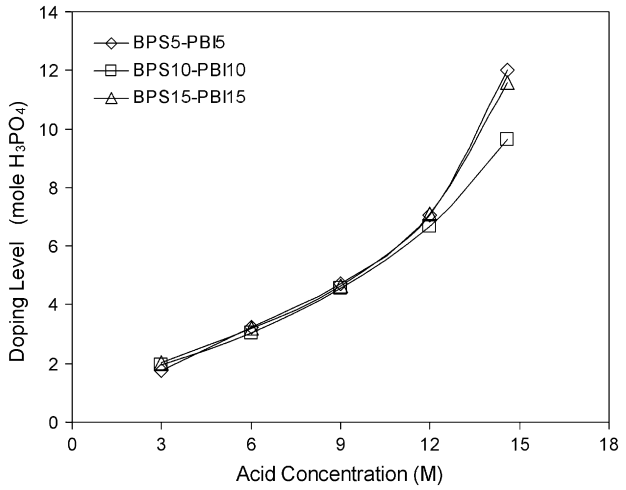

Fig. 13. Phosphoric acid doping level of BPS–PBI membranes as a function of the acid concentration with different block lengths.

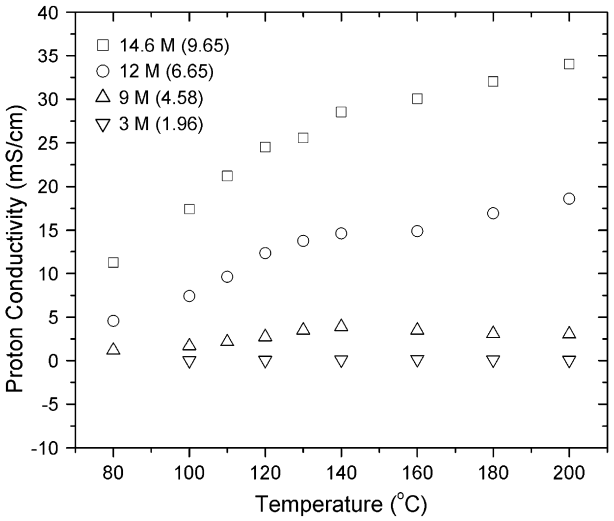

Fig. 15. Influence of temperature on ionic conductivity for BPS10–PBI10 samples at varying phosphoric acid doping levels.

Table 3
Swelling ratios of BPS–PBI and PBI homopolymer membranes doped with H_3PO_4 solution for 72 h

Copolymers	Length (%)	Thickness (%)	Volume (%)	Acid Conc. for doping (M)	Acid in sample (wt.%)
PBI[a]	22.7	105.5	209	14.6	78.8
PBI[a]	9.5	95.5	134	12.0	60.9
BPS 5–PBI 5	2.7	60.0	69	14.6	63.5
BPS 10–PBI 10	2.7	42.9	51	14.6	59.2
BPS 15–PBI 15	1.7	56.3	62	14.6	62.6

[a] Intrinsic viscosity in NMP at 25 °C was 2.35 dL g^{-1}.

Table 4
Mechanical Properties of BPS15–PBI15 with different doping levels

Doping level	Acid in sample (wt.%)	Modulus (MPa)	Stress at break (MPa)	Elongation at break (%)
0	0	2880 ± 100	73 ± 3	10 ± 2
4.6	40.0	860 ± 60	46 ± 5	149 ± 12
11.5	62.6	440 ± 80	31 ± 6	205 ± 16

doped with lower acid concentrations (3 and 9 M), the doping levels ranged from 4 to 5. As the theoretical number of "bound" phosphoric acid units is 4, ionic conduction at this doping level can occur only through proton hopping between the N–H site and the phosphate anion [23]. However when the membranes were doped with higher acid concentrations (12 and 14.6 M), the doping levels were between 6 and 12 and the presence of "free" phosphoric acid or the quickly diffusing $H_2PO_4^-$ anions increases the ionic conductivity significantly.

Ionic conductivity measured as a function of temperature also showed an increasing trend for all samples. However, a change in slope was observed above 150 °C, which may be attributed to a change in the conduction mechanism. It is known that "fused" phosphoric acid can be formed from the "free" phosphoric acid at high temperatures and so the slope change may indicate a transition from a hopping mechanism to a vehicle mechanism involving bodily diffusion of protons as proposed by Hayamizu et al. [23]. The activation energy for ionic transport was determined for all samples over the temperature range of 100–150 °C. The activation

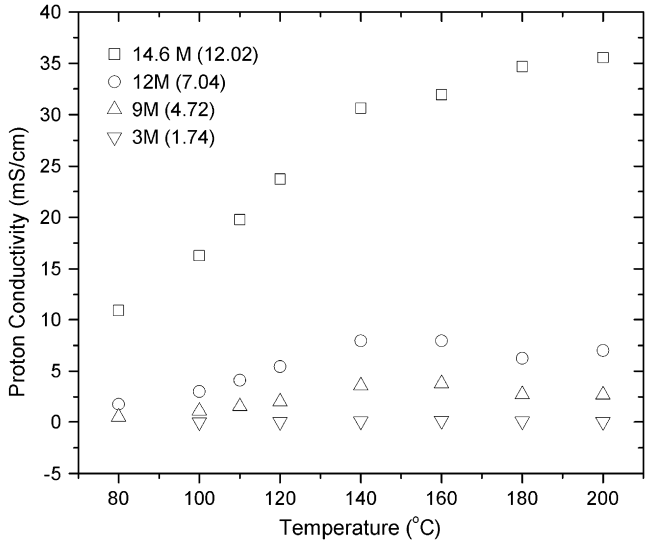

Fig. 14. Influence of temperature on ionic conductivity for BPS5–PBI5 samples at varying phosphoric acid doping levels.

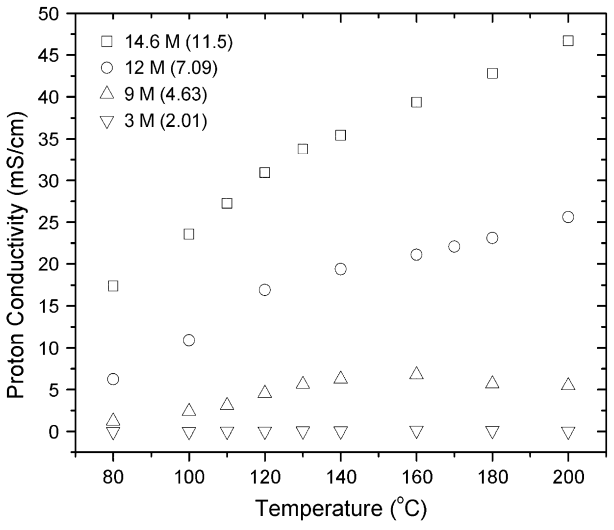

Fig. 16. Influence of temperature on ionic conductivity for BPS15–PBI15 samples at varying phosphoric acid doping levels.

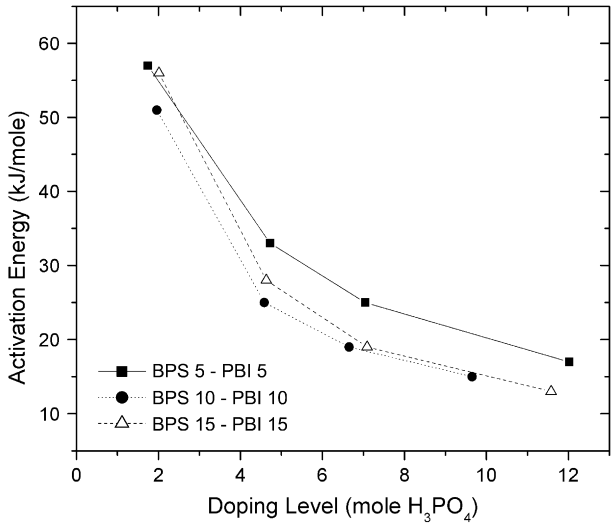

Fig. 17. Influence of phosphoric acid content on activation energy.

energy calculated showed a strong dependency on doping level as shown in Fig. 17. A significant drop in activation energy from 60 to 20 kJ/mole was observed for BPS15–PBI15 sample as the doping level was increased from 2 to 6. A similar trend was also seen in BPS5–PBI5 and BPS10–PBI10 samples. This sharp decrease can be attributed to the involvement of the free phosphoric acid or the phosphate anion in the transport process. A further increase in phosphoric acid content resulted in a nominal decrease in the activation energy value.

Among the copolymers, the highest conductivity at 200 °C was 47 mS/cm from BPS15–BPS15 with a doping level of 11.5. This value is relatively low when compared to the current record conductivity of 250 mS/cm at 200 °C which was acquired with the phosphoric acid doped PBI membrane via the sol–gel process [19]. However, considering the sol–gel processed membrane's doping level is extraordinarily high (e.g., 20–40), the ionic conductivity of 47 mS/cm with the doping level of 11.5 is reasonable.

It is worthwhile to compare ionic conductivities of the multiblock copolymer system and conventional PBI system with similar acid contents instead of doping levels. Since the PBI compositions of the multiblock copolymers are around half of the system, at the same doping level, the acid contents in the multiblock copolymers will be much lower than those of homopolymer PBI. For example, the weight based acid content in BPS15–PBI15 (PBI composition 45%) with a doping level of 11.5 will be the same as that of conventional PBI system with a 5.18 doping level. Previously, Litt et al., reported ionic conductivity of the conventional phosphoric acid doped PBI system with 5.01 doping level. The ionic conductivities ranged from 25 to 40 mS/cm with 5–10% relative humidity (RH) at 190 °C [16].

3.6. Influence of the microstructure of the multiblocks on the ionic transport

Over the last few years, our group has been investigating the influence of morphology on proton transport of sulfonic acid containing multiblock copolymers as a function of relative humidity (RH). The proton conductivity under partially hydrated conditions was found to increase with increasing block length or with the extent of phase separation [36]. In the current investigation with the selectively doped BPS–PBI system, ionic conductivity was studied as a function of doping level at 140 °C. The three copolymers with varying block lengths were compared as shown in Fig. 18. Among the copolymers, the conductivities of BPS15–BPS15 and BPS10–BPS10 showed a similar trend with doping level in contrast to BPS5–PBI5 sample. This suggests a morphological change from BPS5–BPS5 sample to BPS10–BPS10 sample. At a given doping level, the ionic conductivity was found to increase with increasing block length. The effect was more pronounced at lower doping levels (6–7). This can be attributed to the formation of a phase separated morphology with increasing block lengths as indicated by the DMA study. The phase separated morphology resulted in improved connectivity within the PBI units. This is consistent with our earlier findings with the sulfonic acid containing multiblock copolymers. The increased connectivity with block length is expected to lower the morphological barrier for ion transport with increased ionic conductivity. Thus by synthesizing phase separated multiblock copolymers, improved ionic conductivity can be achieved with lower phosphoric acid doping levels.

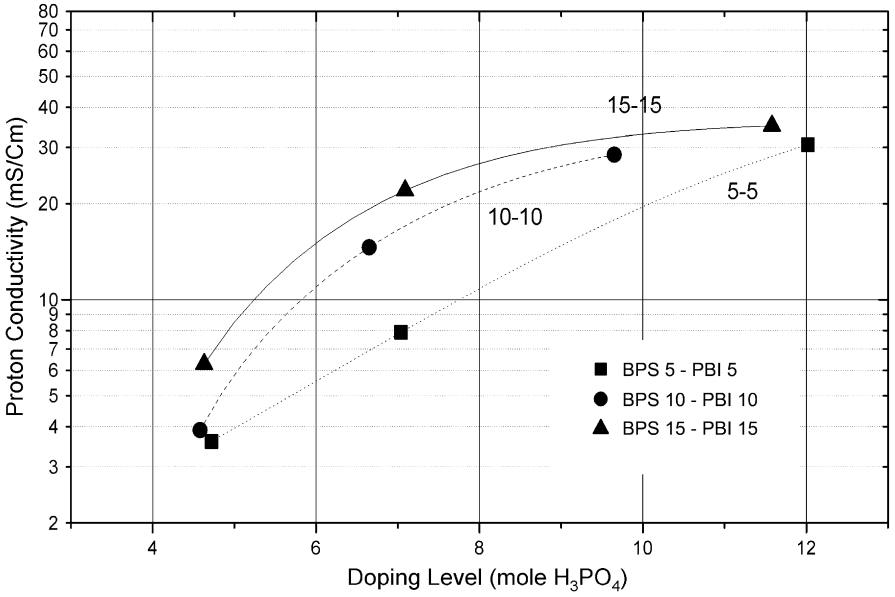

Fig. 18. Influence of block length on ionic conduction with varying phosphoric acid doping level at 140 °C.

4. Conclusions

A novel thermally stable multiblock copolymer system was developed and characterized for low humidity high temperature PEM applications. The multiblock copolymers were synthesized via a coupling reaction between telechelic carboxyl functional poly(arylene ether sulfone) and *o*-diamine-terminated polybenzimidazole. Transparent and ductile membranes were prepared by solvent casting from DMAc and two distinct T_gs were observed by DMA. The ionic conduction of the membranes was achieved by immersing the membranes in H_3PO_4 solution. A doping level and water uptake study revealed that the doping levels of the membranes strongly depend on the concentration of H_3PO_4 doping solution while the water uptake has a limited influence. The ionic conductivity study revealed that there was a strong dependency on temperature, doping level and more importantly the microstructure of the samples. The ionic conductivity was found to increase significantly after a particular doping level for all the copolymers and was attributed to the appearance of "free" phosphoric acid. At a given doping level, the ionic conductivity was found to increase with increasing block length. The formation of the phase separated morphology with increasing block length was confirmed by DMA analysis. The increased phase separation resulted in better connectivity and improved ion transport. Future research will further clarify morphology via transmission electron microscopy and scattering methodologies. Mechanical properties will also be compared to PBI homopolymers. Exploration of applications for these materials in gas separation and reverse osmosis, as well as fuel cell testing for MEA fabrication and catalyst durability will also be pursued.

The authors thank the Department of Energy (DE-FG36-06G016038) for its support of this research.

References

[1] Savadogo O. Journal of New Materials for Electrochemical Systems 1998;1(1):47–66.
[2] Kreuer KD. Journal of Membrane Science 2001;185(1):29–39.
[3] Banerjee S, Curtin DE. Journal of Fluorine Chemistry 2004;125(8):1211–6.
[4] Hamrock SJ, Yandrasits MA [Philadelphia, PA, United States]. Polymer Reviews 2006;46(3):219–44.
[5] Kim YS, Dong L, Hickner MA, Glass TE, Webb V, McGrath JE. Macromolecules 2003;36(17):6281–5.
[6] Kreuer KD, Rabenau A, Weppner W. Angewandte Chemie 1982;94(3):224–5.
[7] Kim YS, Wang F, Hickner M, Zawodzinski TA, McGrath JE. Journal of Membrane Science 2003;212(1−2):263–82.
[8] Hill ML, Kim YS, Einsla BR, McGrath JE. Journal of Membrane Science 2006;283(1 + 2):102–8.
[9] Costamagna P, Yang C, Bocarsly AB, Srinivasan S. Electrochimica Acta 2002;47(7):1023–33.
[10] Hickner MA, Ghassemi H, Kim YS, Einsla BR, McGrath JE [Washington, DC, United States]. Chemical Reviews 2004;104(10):4587–611.
[11] He R, Li Q, Xiao G, Bjerrum NJ. Journal of Membrane Science 2003;226(1–2):169–84.
[12] Steininger H, Schuster M, Kreuer KD, Kaltbeitzel A, Bingoel B, Meyer WH, et al. Physical Chemistry Chemical Physics 2007;9(15):1764–73.
[13] Sammes N, Bove R, Stahl K. Current Opinion in Solid State and Materials Science 2005;8(5):372–8.
[14] Kongstein OE, Berning T, Borresen B, Seland F, Tunold R [Oxford, United Kingdom]. Energy 2006;32(4):418–22.
[15] Lobato J, Canizares P, Rodrigo MA, Linares JJ. Electrochimica Acta 2007;52(12):3910–20.
[16] Wainright JS, Wang JT, Weng D, Savinell RF, Litt M. Journal of the Electrochemical Society 1995;142(7):L121–3.
[17] Xiao L, Zhang H, Choe E-W, Scanlon E, Ramanathan LS, Benicewicz BC. Preprints of Symposia – American Chemical Society, Division of Fuel Chemistry 2003;48(1):447–8.
[18] Li Q, He R, Berg RW, Hjuler HA, Bjerrum NJ. Solid State Ionics 2004;168(1–2):177–85.
[19] Xiao L, Zhang H, Scanlon E, Ramanathan LS, Choe E-W, Rogers D, et al. Chemistry of Materials 2005;17(21):5328–33.
[20] van Grotthuss CJD. Ann Chim 1806;58:54.
[21] Agmon N. Chemical Physics Letters 1995;244(5(6)):456–62.
[22] Hughes CE, Haufe S, Angerstein B, Kalim R, Maehr U, Reiche A, et al. Journal of Physical Chemistry B 2004;108(36):13626–31.
[23] Aihara Y, Sonai A, Hattori M, Hayamizu K. Journal of Physical Chemistry B 2006;110(49):24999–5006.
[24] Li Q, He R, Jensen JO, Bjerrum NJ. Fuel Cells (Weinheim, Germany) 2004;4(3):147–59.
[25] Xu H, Chen K, Guo X, Fang J, Yin J. Journal of Polymer Science, Part A: Polymer Chemistry 2007;45(6):1150–8.
[26] Li Q, Pan C, Jensen JO, Noye P, Bjerrum NJ. Chemistry of Materials 2007;19(3):350–2.
[27] Staiti P, Minutoli M. Journal of Power Sources 2001;94(1):9–13.
[28] Harrison WL, Hickner MA, Kim YS, McGrath JE [Weinheim, Germany]. Fuel Cells 2005;5(2):201–12.
[29] Kim YS, Hickner MA, Dong L, Pivovar BS, McGrath JE. Journal of Membrane Science 2004;243(1–2):317–26.
[30] Lee H-S, Badami AS, Roy A, McGrath JE. Journal of Polymer Science, Part A: Polymer Chemistry 2007;45(21):4879–90.
[31] Wang H, Badami AS, Roy A, McGrath JE. Journal of Polymer Science, Part A: Polymer Chemistry 2006;45(2):284–94.
[32] Lee H-S, Roy A, Badami AS, McGrath JE. PMSE Preprints 2006;95:210–1.
[33] Ghassemi H, Ndip G, McGrath JE. Polymer 2004;45(17):5855–62.
[34] Lee H-S, Roy A, Lane O, Dunn S, McGrath JE. Polymer 2008;49(3):715–23.
[35] Cooper KL. Dissertation. Virginia Polytechnic Institute and State University; 1991.
[36] Roy A, Hickner MA, Yu X, Li Y, Glass TE, McGrath JE. Journal of Polymer Science, Part B: Polymer Physics 2006;44(16):2226–39.